Characterization and Application of Nanomaterials 2024, 7(2), 7007.
https://doi.org/10.24294/can.v7i2.7007

Article

Ajwa date seed mediated green synthesis of alginate-silver nanocomposite beads and films for antibacterial and catalytic degradation applications

Naba Almukharraq[†], Marwa Almarzooqi[†], Hasan Ruyan[†], Fatima AlHannan, Praveen Kumar, Fryad Henari, G. Roshan Deen[*]

Materials for Medicine Research Group, School of Medicine, Royal College of Surgeons in Ireland (RCSI), Medical University of Bahrain, Busaiteen 228, Kingdom of Bahrain

*** Corresponding author:** G. Roshan Deen, rdeen@rcsi.com

[†] Equal contribution to this work and share first author status.

CITATION

Almukharraq N, Almarzooqi M, Ruyan H, et al. Ajwa date seed mediated green synthesis of alginate-silver nanocomposite beads and films for antibacterial and catalytic degradation applications. Characterization and Application of Nanomaterials. 2024; 7(2): 7007. https://doi.org/10.24294/can.v7i2.7007

ARTICLE INFO

Received: 11 June 2024
Accepted: 3 July 2024
Available online: 1 August 2024

Abstract: Alginate-silver nanocomposites in the form of spherical beads and films were prepared using a green approach by using the aqueous extract of Ajwa date seeds. The nanocomposites were fabricated by in situ reduction and gelation by ionotropic crosslinking using calcium ions in solution. The rich phytochemicals of the date seed extract played a dual role as a reducing and stabilizing agent in the synthesis of silver nanoparticles. The formation of silver nanoparticles was studied using UV-Vis absorption spectroscopy, and a distinct surface plasmon resonance peak at 421 nm characteristic of silver nanoparticles confirmed the green synthesis of silver nanoparticles. The morphology of the nanocomposite beads and film was compact, with an even distribution of silver nanoclusters. The catalytic property of the nanocomposite beads was evaluated for the degradation of 2-nitrophenol in the presence of sodium borohydride. The degradation followed pseudo-first-order kinetics with a rate constant of 1.40×10^{-3} s^{-1} at 23 °C and an activation energy of 18.45 kJ mol^{-1}. The thermodynamic parameters, such as changes in enthalpy and entropy, were evaluated to be 15.22 kJ mol^{-1} and −197.50 J mol^{-1} K^{-1}, respectively. The nanocomposite exhibited properties against three clinically important pathogens (gram-positive and gram-negative bacteria).

Keywords: Ajwa dates seed; silver nanoparticles; green synthesis; alginate beads; degradation; 2-nitrophenol; antibacterial activities

1. Introduction

Water contamination from toxic organic chemical waste from pharmaceutical, textile, and electrochemical industries and their adverse effects on human and aquatic life have received tremendous attention in recent years. Exposure to chemicals above the threshold limits leads to skin discoloration, damage to the nervous system and organs, and developmental effects [1]. The toxic chemicals include nitrophenols, azo dyes, and heavy metals, and water containing these needs to be treated before it is safely discharged into waterbodies or land. Various approaches have been employed in the removal of harmful pollutants, such as adsorption, ion exchange, solvent extraction, photochemical reactions, etc. [2], and among these techniques, adsorption using activated carbon is widely used as the process is economical and effective in the removal of various pollutants. However, this method allows for the adsorption of pollutants but not their degradation to non-toxic substances.

In recent years, photocatalysis or photodegradation methods using metallic and metal oxide nanoparticles such as silver, gold, platinum, palladium, copper, nickel,

cobalt, iron, zinc oxide (ZnO), and titanium dioxide (TiO_2) have gained much research attention for the complete reduction of toxic chemical waste to non-toxic substances in water [3–7]. Nanoparticles on solid polymer supports such as polysulfone, polypropylene, poly(vinylidene fluoride), polyamide, cellulose acetate, and sodium alginate offer improved catalytic properties along with material sustainability, as these materials can be used repeatedly [7–9]. Silver nanoparticles supported on various inorganic and organic substrates such as zeolite, silica or fiber glass, carbon materials, natural macro-porous materials, and polymers have been recognized as effective photocatalysts and antimicrobial agents. Nanocomposite beads based on the natural polymers sodium alginate and silver nanoparticles offer extended physical and chemical properties and are currently being considered for point-of-use drinking water disinfection [8–10].

Sodium alginate is a linear polysaccharide found in marine brown algae and is composed of irregular blocks of b-D-mannuronic acid (M) and a-L-guluronic residues (G). Due to their non-toxicity, degradability, and bio-compatibility alginate-based gels have attracted numerous biomedical applications, such as drug and protein delivery, wound dressing, 3D bioprinting for tissue engineering, scaffolds for cell growth and organoid morphogenesis, and flexible electronics for health monitoring [11–15].

Silver nanoparticles synthesized by green chemistry using the extracts of plants or plant products have been used in the fabrication or engineering of alginate-nanocomposite beads. The phytochemicals present in the extract act both as reducing agents for the reduction of silver salt to silver nanoparticles and as stabilizing the resulting nanoparticles against aggregation [16,17]. Date palm, commonly known as *Phoenix dactylifera*, is one of the oldest cultivated varieties of date palm trees with nutritional, economic, and environmental benefits. There are about 5000 varieties of date palm that are grown in different regions of the world, and the nutritional and phytochemical values vary among the dates. Among these, Ajwa dates are widely cultivated in the Al Madinah and surrounding regions of Saudi Arabia. This type of date has high sugar (34.5% glucose, 25.6% fructose, and 0.5% sucrose) and mineral (3%) content compared to other varieties of dates [18,19]. These date seeds are a rich source of polyphenols, flavonoids, glycosides, phenolic acids, proteins, and carbohydrates and demonstrate antioxidant, anti-inflammatory, antimicrobial, and anti-tumor properties. The extract of the Ajwa date seed in methanol and acetone exhibits reasonable antibacterial properties against gram-positive and gram-negative bacteria [19,20].

In this study, we have developed reusable alginate-based silver nanocomposite beads by in situ chemical reduction and gelation methods for the quick reduction of 2-nitrophenol. The silver nanoparticles were first synthesized by green chemistry using the extract of Ajwa date seeds as an efficient source for reduction and stabilization, and then incorporated into alginate beads by ionotropic crosslinking using calcium ions. To the best of our knowledge, this is the first study on the fabrication of alginate-silver nanocomposite beads using the extracts of Ajwa date seed.

2. Experimental

2.1. Materials

Ajwa date (*Phoenix dactylifera*) seed powder was purchased from a grocery store in Hoora, Bahrain. Silver nitrate ($AgNO_3$), sodium alginate ($NaC_6H_7O_6$), sodium hydroxide (NaOH), sodium borohydride ($NaBH_4$), 2-nitrophenol (2-NP), Congo red (CR), and calcium chloride ($CaCl_2$) were purchased from sigma and used as received. Deionized water collected from a Millipore system (Elix Technology, Germany) with a conductivity of 18.2 MW cm^{-1} was used for all aqueous sample preparations. The antibacterial properties of the synthesized nanoparticles, nanocomposite beads, and films were evaluated against three different types of bacteria: *Staphylococcus aureus* (*S. aureus*), *Escherichia coli* (*E. coli*), and *Salmonella typhimurium* (*S. typhimurium*). The bacteria were obtained from the Ministry of Health, Kingdom of Bahrain (MOH, Bahrain, Microbiologiscs, France).

2.2. Preparation of date seeds extract

About 1.00 g of the date seed powder was added to 100 mL of water in a beaker and boiled for 30 min under magnetic stirring. The mixture was air-cooled and centrifuged for 10 min at an rpm of 4200 to remove any suspended materials. The clear extract was used fresh in the synthesis of silver nanoparticles.

2.3. Green synthesis of silver nanoparticles

Silver nanoparticles were synthesized by reducing the silver nitrate in the freshly prepared date seed extract as follows: $AgNO_3$ (1 mm, 5 mL) was placed in a screw-capped glass vial and stirred gently using a magnetic stirring bar. Freshly prepared date seed extract (1 mL) was added dropwise into the vial with continuous stirring. After about 5 min, NaOH (0.5 M, 50 mL) was added dropwise, and the mixture was stirred overnight for the completion of the reaction. Upon addition of NaOH, the color of the solution turned pale yellow and finally to brown (after 24 h). The observed color changes are an indication of the formation of nanoparticles. The solution containing the nanoparticle was centrifuged (rpm 10,000) for 10 min, and the sedimented nanoparticles were washed repeatedly with water and dried in an oven at 70 ℃.

2.4. Synthesis of alginate-silver nanocomposite beads

Alginate beads containing silver nanoparticles were prepared by the sequential chemical reduction and gelation method as described as follows: In this method, silver nanoparticles were first synthesized using the date seed extract and then incorporated into the alginate beads during the gelation. A silver nitrate solution of concentration 1 mm was first prepared by dissolving 0.0175 g of the salt in 100 mL of water. To this solution, 20 mL of fresh date seed extract was added under magnetic stirring, followed by the addition of 1 mL of 0.5 M NaOH. Upon addition of sodium hydroxide, the solution turned pale gray and then pale brown, indicating the onset of the formation of silver nanoparticles. The solution was continuously stirred for an additional 24 h for the completion of the reaction, followed by the

addition of 2.20 g of sodium alginate. The solution was heated to 60 ℃ and continuously stirred for another 24 h for the complete dissolution of sodium alginate, resulting in a homogenous mixture. The solution was air-cooled and then stored in the refrigerator to remove any air bubbles. The prepared alginate-silver nanoparticle solution was injected into 200 mL of a 5 wt% calcium chloride solution using a plastic syringe of 20 mL capacity at a rate of 20 drops per minute. The resulting black-colored beads were washed thoroughly with water and dried at 70 ℃ until a constant weight was maintained.

2.5. Synthesis of peelable alginate-silver nanocomposite films

Peelable alginate-silver nanocomposite film was prepared by a mist spray gelation method as described as follows: A 10 mL alginate-silver nanoparticle solution described in the previous section was placed in a clean glass petri dish and mist sprayed with $CaCl_2$ solution (5 wt%). The petri dish was covered and left overnight at room temperature for the completion of gelation. The dark brown film was carefully peeled off from the petri dish, washed repeatedly with water, and dried at 50 ℃ until a constant weight was maintained.

2.6. UV-Vis absorption spectroscopy

The formation of silver nanoparticles was confirmed by measuring the absorbance of the silver nanoparticle solution using a double-beam Shimadzu UV-1800 spectrophotometer. The solution (3 mL) was placed in a quartz cuvette (Helma) of 1 cm path length, and the absorption spectrum was recorded in the wavelength range 250–1000 nm with a resolution of 1 mm. Water was used as the blank reference for all measurements.

2.7. Scanning electron microscopy (SEM)

The size and morphology of the alginate-silver nanocomposite beads were characterized using a scanning electron microscope operating at a voltage of 10 kV (Inovenso, IEM-11). The samples were sputtered with gold for 15 s using an Inovenso SPT-20 coater.

2.8. Catalytic degradation studies of 2-nitrophenol (2-NP)

The catalytic degradation of 2-NP by the alginate-silver nanocomposite beads was followed using a UV-Vis spectrophotometer. A solution of 2-NP (0.13 mm, 2.5 mL) was placed in a quartz cuvette of 1 cm path length, and the absorbance was recorded. After this, 0.5 mL of freshly prepared $NaBH_4$ (0.1 M) was added to the solution, and the absorbance was recorded again. About 10 nanocomposite beads were then added to the solution, and the change in absorbance was recorded at intervals of 3 min for a period of 15 min. The percentage degradation of 2-NP was calculated using the following equation,

$$\text{Degradation (\%)} = \frac{A_0 - A_t}{A_0} \times 100 \quad (1)$$

where, A_0 and A_t are the absorbance at time zero and absorbance at time *t*, respectively.

2.9. Antibacterial activity

The antibacterial activity of the synthesized silver nanoparticles against different types of gram-positive and gram-negative bacteria, such as *S. aureus*, *E. coli*, and *S. typhimurium*, was carried out using the Kirby-Bauer disk diffusion susceptibility test method. The bacteria strains were spread on a nutrient agar (LB agar) medium using a sterile spreader in all directions. The filter paper discs were loaded with silver nanoparticles with aseptic precautions, and then the agar plate was incubated at 37 ℃ for 24 h. The zone of inhibition was observed and measured after 24 h of incubation.

3. Results and discussion

3.1. Ajwa date seeds mediated green synthesis of silver nanoparticles

Plant extract-mediated synthesis of metallic nanoparticles is a desired method as it is environmentally friendly and toxic reagents are not used in the process. The formation of silver nanoparticles using the aqueous extract of Ajwa date seeds was studied by visual observation and spectrophotometry. Upon the addition of the date seed extract to the silver nitrate solution, a color change to pale brown was observed, which indicates the in situ chemical reduction of silver ions (Ag^{+}) to silver nanoparticles (Ag^{0}). The formation of silver nanoparticles was quantified using UV-Vis absorption spectroscopy, and a distinct surface plasmon resonance (SPR) peak centered at 421 nm confirmed the presence of silver nanoparticles in the solution, as shown in **Figure 1**.

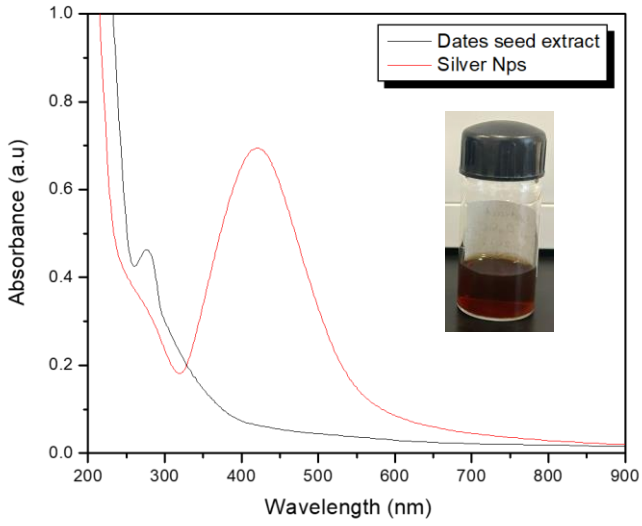

Figure 1. UV-Vis absorption spectra of colloidal silver nanoparticles synthesized using Ajwa dates seeds (insert: digital image of colloidal silver nanoparticles).

This peak arises due to collective oscillations of conduction electrons in the electromagnetic field of the incident light [16,17]. The Ajwa date seeds are rich in phytochemicals such as polyphenols, flavonoids including rutin, catechins, iso-flavonoids, and lignans [18–20]. These phytochemicals present in the extract of Ajwa date seeds are responsible for the chemical reduction and subsequent

stabilization of the resulting silver nanoparticles. The peak at 276 nm for the date seeds is attributed to the active phytochemicals that are responsible for the chemical reduction. The absence of this peak in the spectrum of the silver nanoparticles correlates to the reaction and the reduction in concentration of the active phytochemical. The nanoparticles were stable against aggregation for more than a month, with no obvious change in the position (401 nm) and intensity of the SPR peak observed in the absorption spectrum.

3.2. Formation and morphology of alginate beads and film

Silver particles encapsulated in alginate beads were prepared by ionotropic crosslinking with divalent cations such as calcium ions (Ca^{2+}). The divalent cations bind to the guluronate blocks of the sodium alginate chains, as the blocks allow a high degree of coordination with the cations. The guluronate blocks of one polymer then form physical junctions (crosslink points) with the guluronate blocks of adjacent polymer chains. This type of crosslinking and formation of a gel is termed the egg-box model of crosslinking [21].

The alginate beads containing silver particles prepared in this study were pale brown in color in their hydrated state and black when completely dry, as shown in **Figure 2a**,**b.** The dry beads were close to spherical in shape, with an average size of 1.2 mm, as shown by the SEM micrograph in **Figure 2c**. The surface of the nanocomposite beads was compact, with dense particulate clusters of silver in the form of plates (**Figure 2d**). To verify the presence of silver nanoparticles, the alginate beads were soaked in a phosphate buffer solution and dissociated.

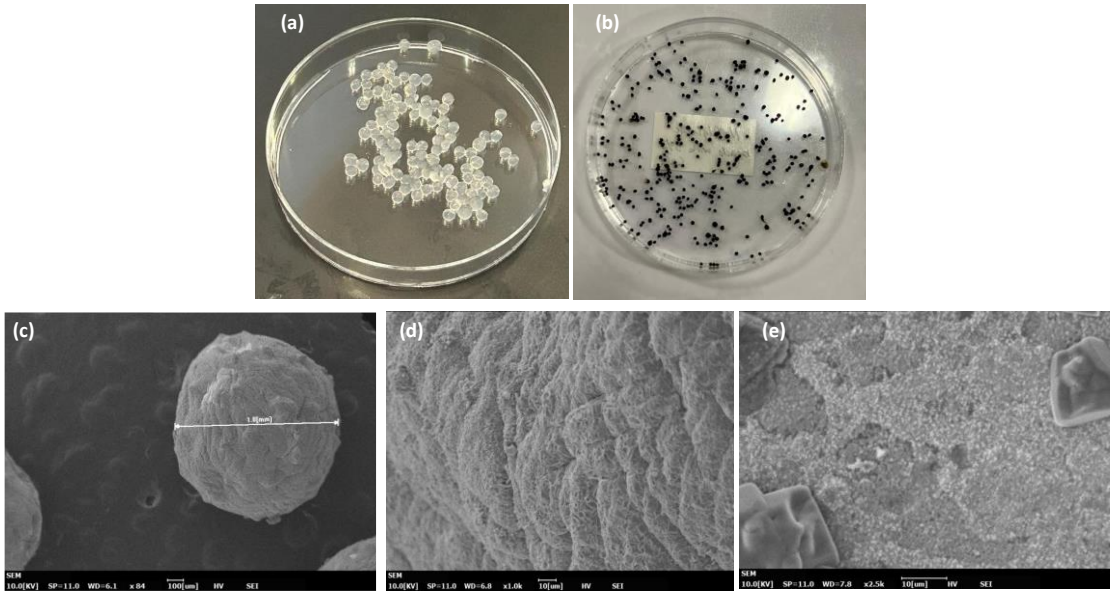

Figure 2. Images of alginate beads; **(a)** wet alginate beads; **(b)** dry alginate-silver nanocomposite beads; **(c)** SEM image of nanocomposite bead; **(d)** high magnification SEM image of nanocomposite bead; **(e)** SEM image of nanocomposite film.

The dissociation causes chelation of Ca^{2+} by PO_4^- and HPO_4^{2-} ligands, releasing the alginate and silver nanoparticles in solution. The resulting viscous solution was analyzed by UV-Vis absorption spectroscopy. A strong SPR peak around 420 nm

confirmed the presence of silver nanoparticles in the alginate-nanocomposite beads. The nanocomposite film does not show any significant morphology, and the silver nanoparticles were evenly distributed on the surface of the film, as observed in **Figure 2e**.

3.3. Catalytic degradation of 2-nitrophenol (2-NP)

Effluents from the dye and pesticide industries contain 2-NP, which is an environmental hazard and is known to cause methemoglobinemia. The reduced product of 2-NP is 2-amino phenol (2-AP), which is a non-toxic product. The catalytic activity of the alginate-silver nanocomposite beads in the degradation of 2-NP in the presence of $NaBH_4$ was studied using UV-Vis absorption spectroscopy. The time-dependent change in absorbance during the degradation of 2-NP is shown in **Figure 3a**. The absorption peak at 351 nm corresponds to 2-NP, and this shifts to 416 nm due to the formation of a 2-nitrophenolate ion (due to deprotonation of the −OH group) upon the addition of $NaBH_4$ as observed in **Figure 3a**. The reduction in the absorption of the 2-nitrophenolaote ion corresponds to the formation of 2-AP; however, this reaction has a large kinetic barrier due to the large potential difference between the reducing agent ($NaBH_4$) and 2-NP [22]. As a result, a catalyst is required to overcome the large energy barrier associated with this reduction process at room temperature.

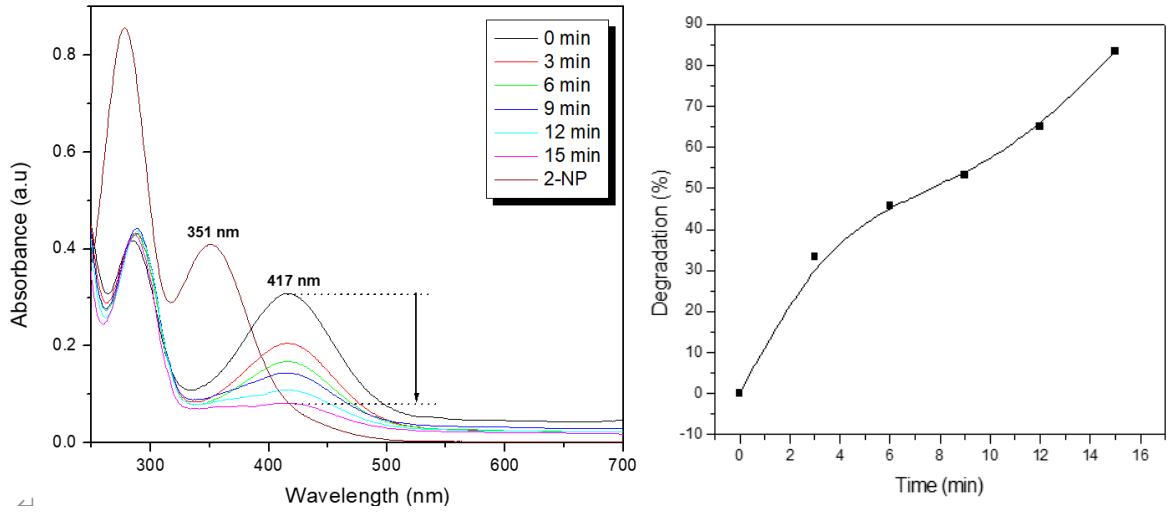

Figure 3. Degradation of 2-NP in the presence of alginate-silver nanocomposite beads in the presence of $NaBH_4$; **(a)** UV-Vis absorption spectra showing the degradation; **(b)** plot of percent degradation as function of reaction time.

Upon addition of the nanocomposite beads (10 beads) into the solution, the initial absorption (0.30) at 416 nm decreased significantly, reaching 0.05 in 15 min. This decrease corresponds to about 83% of the of the degradation of 2-NP. At the same time, the intensity of the absorption peak at 300 nm increased, which indicates the formation of 2-AP and the reaction being accelerated by the silver nanoparticles present in the nanocomposite. The degradation kinetics are shown in **Figure 3b**, and a degradation of 83% is observed in just 15 min of the reaction.

The rate of reaction could be shortened by improving the surface morphology of the nanocomposite beads by making them more porous, which would allow higher diffusion of the 2-nitrophenolate ion into the beads for a faster reaction with the active proton species, or by increasing the number of beads. In the absence of the nanocomposite beads, the degradation reaction was extremely slow (more than 3 days), confirming the major catalytic role of the silver nanoparticles. The degradation reaction mechanism [21–23] in the presence of the nanocomposite takes place in four steps, such as: (i) adsorption of 2-NP onto the nanocomposite bead; (ii) diffusion of 2-NP to the active site; (iii) reaction of 2-NP to form the adsorbed product; and (iv) desorption of the product from the nanocomposite. A schematic representing the degradation of 2-NP in the presence of the strong reducing agent, $NaBH_4$, is shown in **Figure 4**, according to literature reports [22,23].

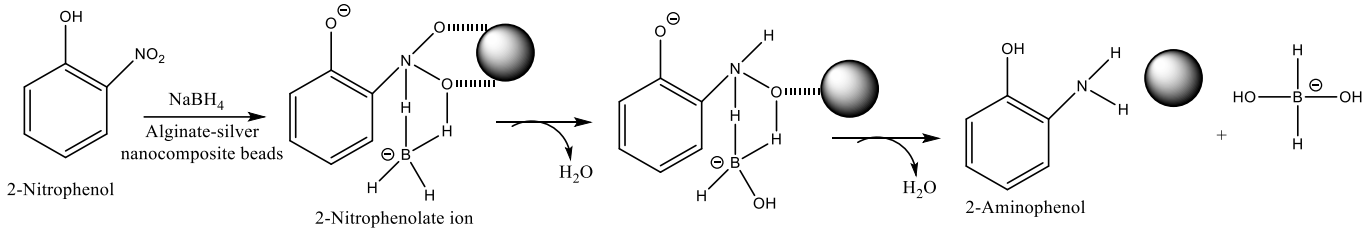

Figure 4. Mechanism of degradation of 2-NP in the presence of alginate-silver nanocomposite beads and $NaBH_4$.

The rate constant (k) of the degradation was determined from the linear plot of $\ln(A_t/A_0)$ versus reaction time (t) in min (**Figure 5**) according to the following linear equation,

$$\ln\frac{C_t}{C_0} = \ln\frac{A_t}{A_0} = -kt \quad (2)$$

where C_t and C_0 are the concentration of 2-NP, and A_t and A_0 are the absorbances at time t, and $t = 0$, respectively, k (min^{-1}) is the rate constant of the reaction.

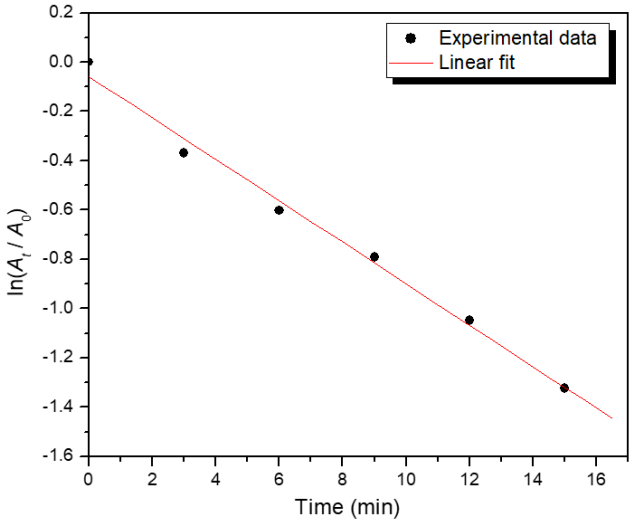

Figure 5. Plot of $\ln(A_t/A_0)$ versus time for the reduction of 2-NP in the presence of $NaBH_4$ at 23 °C.

The degradation reaction follows a pseudo-first order reaction kinetics with

respect to the alginate-silver nanocomposite beads because the concentration of $NaBH_4$ (10 mm) was much higher than that of 2-NP (1 mm). The rate constant for the degradation reaction was determined to be 1.40×10^{-3} s^{-1}. The reaction kinetics and the rate constant obtained agree with reported values for catalytic reduction of nitrophenol compounds by green synthesized silver and gold nanoparticles and polymer nanocomposites [21,23–25].

3.4. Catalytic performance of alginate-silver nanocomposite beads

The activation energy (E_a) for the degradation process was determined from the gradient of a plot of ln(k) versus 1/T according to Arrhenius equation as [26],

$$\ln(k) = \left(\frac{E_a}{R}\right)\frac{1}{T} + \ln(A)$$

where A = frequency factor or Arrhenius constant, R = 8.314 J K^{-1} mol^{-1}, T = absolute temperature in Kelvin, and k = rate constant.

From a linear plot of ln(k) versus 1/T, the E_a and A were determined from the gradient and intercept as 18.45 kJ mol^{-1} and 5.19 s^{-1}, respectively (**Figure 6**).

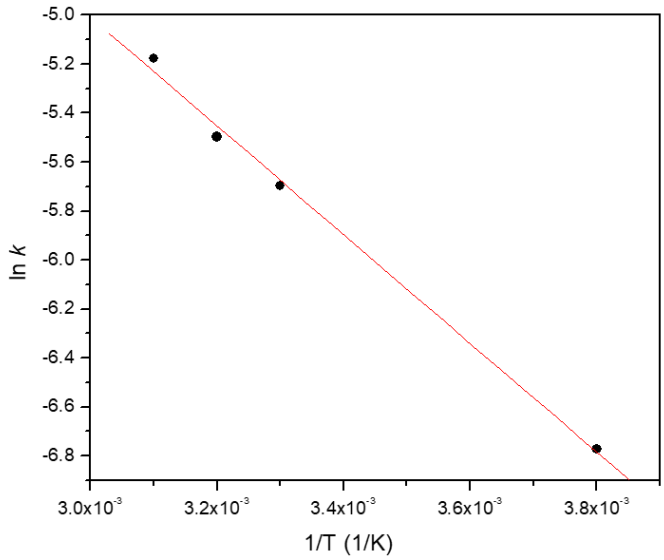

Figure 6. Effect of temperature on the pseudo-first order rate constant and determination of activation energy.

An activation energy of 17 kJ mol^{-1} has been reported for the degradation of 2-NP using calcium alginate beads containing iron-silver bimetallic nanoparticles [5]. Our results agree with this, confirming the excellent catalytic properties of the nanocomposite beads. The results indicate that the catalytic reduction has a low potential barrier and that the catalytic reduction reactions occur via surface catalysis. In comparison to 4-NP (E_a = 10.51 kJ mol^{-1}), the obtained activation energy for 2-NP is higher by a factor of about 1.5, and this increase is attributed to the steric hinderance of 2-NP. The thermodynamic parameters of degradation reaction, such as enthalpy change, (ΔH), and entropy change (ΔS) were determined using the Eyring equation as [5,27],

$$\ln\frac{k}{T} = \ln\frac{k_B}{h} + \frac{\Delta S}{R} - \frac{\Delta H}{R}\left(\frac{1}{T}\right) \quad (3)$$

where k_B is the Boltzmann constant (1.381×10^{-23} JK^{-1}), h is the Planck's constant (6.626×10^{-34} J·s), R is the ideal gas constant, and T is the absolute temperature in Kelvin.

From a linear plot of ln(k/T) versus 1/T (**Figure 7**), the enthalpy (ΔH) and entropy (ΔS) changes for the degradation of 2-NP were determined to be 15.22 kJ mol^{-1} and −197.50 J mol^{-1} K^{-1}, respectively. These values agree with reported values of ΔH = 12.77 kJ mol^{-1} and ΔS = −198.42 J mol^{-1} K^{-1} for the degradation of 2-NP using alginate nanocomposite beads containing iron and silver nanoparticles [5]. The negative entropy values indicate that the randomness on the interface between the nanocomposite bead and 2-NP decreases during the degradation process. The kinetic and thermodynamic parameters for the catalytic reduction of 2-NP by the alginate-silver nanocomposite beads are summarized in **Table 1**.

Table 1. Kinetic and thermodynamic parameters for catalytic degradation of 2-NP by the alginate-silver nanocomposite beads.

Temperature (K)	k (s^{-1})	E_a (kJ mol^{-1})	ΔH (kJ mol^{-1})	ΔS (J mol^{-1} K^{-1})
296	1.400×10^{-3}	18.45	12.77	−198.42
303	3.528×10^{-3}			
308	4.101×10^{-3}			
318	5.650×10^{-3}			

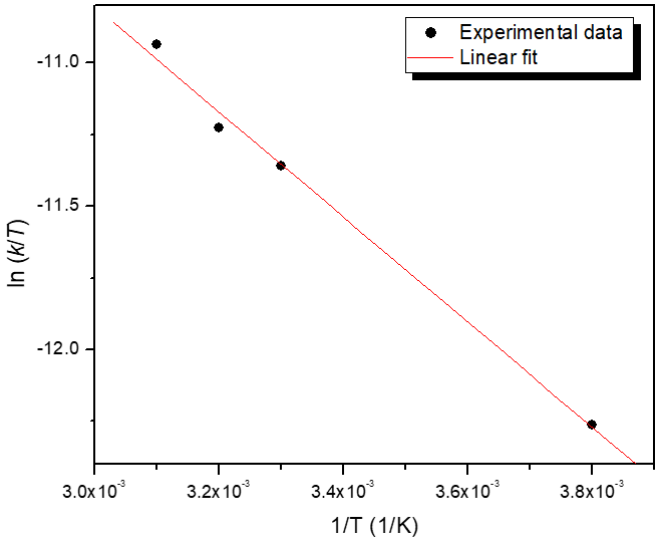

Figure 7. Eyring plot to determine the thermodynamic parameters for the degradation reaction.

The conversion efficiency of the alginate-silver nanocomposite beads was also evaluated for five successive cycles, and the results are shown in **Figure 8**.

After the first cycle of 2-NP degradation, the beads were removed from the solution, washed repeatedly with water, and then placed into a fresh solution containing 2-NP and $NaBH_4$. The conversion efficiency of the nanocomposite beads was constant within the range of 80%–83% up to five successive cycles, which indicates good catalytic efficiency on repeated usage. During this process, no leaching of silver nanoparticles from the beads was observed.

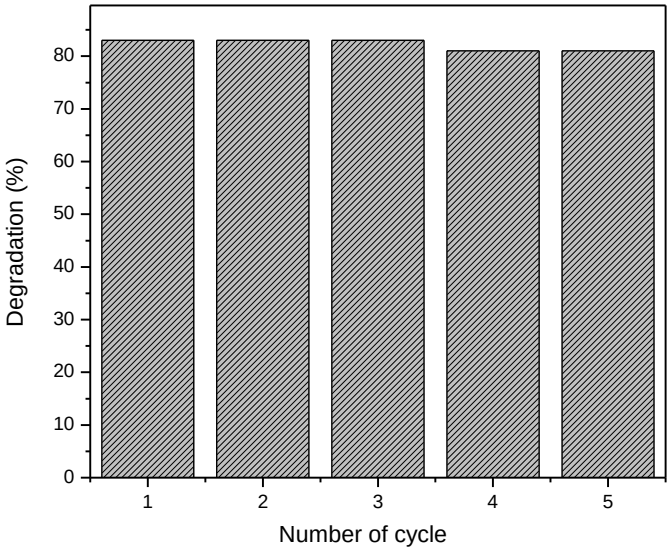

Figure 8. Plot showing the degradation efficiency of the alginate-silver nanocomposite beads for 5 reaction cycles.

3.5. Antibacterial properties

The silver nanoparticles (No. 7), alginate-silver nanocomposite beads (No. 3), and alginate-silver nanocomposite film (No. 2) exhibited weak to good antibacterial properties against *E. coli*, *S. aureus*, and *S. typhimurium*. The bacterial agar plates with the zone of inhibition for a concentration of 10 mm $AgNO_3$ are shown in **Figure 9**. The Ajwa seed extract (No. 5) showed a very weak antibacterial effect against all three types of bacteria, and interestingly, the neat alginate beads (No. 4) showed a comparable effect. The silver nanoparticles (No. 2) were effective against all three types of bacteria, and the antibacterial effect of silver nanoparticles is well known. However, a higher susceptibility was observed for *S. typhimurium*. The alginate-silver nanocomposite beads exhibited a larger zone of inhibition relative to the neat alginate beads, which indicates the synergistic antibacterial effect of the nanocomposites. Similar synergistic effects have been observed for many green-synthesised silver nanocomposites [28].

Figure 9. The antibacterial activity of silver nanoparticles, alginate-silver nanocomposite films and alginate-silver nanocomposite beads on different pathogenic bacteria.

The mechanism of interaction of silver nanoparticles with bacteria is mainly ionic. The silver nanoparticles and silver ions (released from the nanoparticles) can accumulate in the pits of the cell wall, which leads to denaturation of the cell membrane [29]. In addition, the silver nanoparticles could penetrate the cell membrane, leading to denaturation and rupture of organelles, resulting in lysis.

Further, the silver nanoparticles can disrupt bacterial signal transduction, leading to cell apoptosis and the termination of bacterial cell multiplication.

4. Conclusion and future perspectives

Alginate-silver nanocomposites in the form of spherical beads and thin films were successfully fabricated using silver nanoparticles synthesized using the extract of Ajwa date seed. The nanocomposite beads were effective in the catalytic degradation of 2-nitrophenol, and 80% degradation was achieved in 15 min. The beads showed good reusability, with no appreciable decrease in their degradation capacity even after five successive cycles of operation. The degradation followed pseudo-first-order reaction kinetics. The nanocomposite exhibited antibacterial effects against three clinically important pathogens, with a higher susceptibility to *S. typhimurium*. Overall, this study has laid the foundation for a new, effective strategy as an alternative to high-cost commercial catalysis for the detoxification of organic pollutants. The new material developed through the eco-friendly green approach, in addition to its catalytic properties, has the potential to treat hospital wastewater in the future.

Author contributions: Conceptualization, RD; methodology, RD, NA, MA and HR; software, RD; validation, RD and FH; formal analysis, RD, NA and HR; investigation, RD, NA, MA, HR, FA and PK; resources, FA; data curation, RD; writing—original draft preparation, RD; writing—review and editing, RD, NA, MA and HR; supervision, RD and FH; project administration, RD; funding acquisition, RD. All authors have read and agreed to the published version of the manuscript

Conflict of interest: The authors declare no conflict of interest.

Abbreviations

CR	Congo red
NP	2-nitrophenol
SEM	Scanning Electron Microscopy
SPR	Surface Plasmon Resonance
UV-Vis	Ultraviolet-Visible

References

1. Niaz A, Fischer J, Barek B, et al. A novel voltametric method for the determination of maleic acid using silver amalgam paste electrode. Electroanalysis. 2009; 21(15): 1719-1722. doi: 10.1002/elan.200904655
2. Ganapuram BR, Alle M, Dadigala R, et al. Catalytic reduction of methylene blue and Congo red dyes using green synthesized gold nanoparticles capped by Salmalia malabarica gum. International Nano Letters. 2015; 5(4): 215-222. doi: 10.1007/s40089-015-0158-3
3. Gola D, Kriti A, Bhatt N, et al. Silver nanoparticles for enhanced dye degradation. Current Research in Green and Sustainable Chemistry. 2021; 4: 100132. doi: 10.1016/j.crgsc.2021.100132
4. Choudhary MK, Kataria J, Sharma S. Evaluation of the kinetic and catalytic properties of biogenically synthesized silver nanoparticles. Journal of Cleaner Production. 2018; 198: 882-890. doi: 10.1016/j.jclepro.2018.09.015
5. Gupta VK, Yola ML, Eren T, et al. Catalytic activity of Fe@Ag nanoparticle involved calcium alginate beads for the

reduction of nitrophenols. Journal of Molecular Liquids. 2014; 190: 133-138. doi: 10.1016/j.molliq.2013.10.022
6. Augustine R, Kalarikkal N, Thomas S. A facile and rapid method for the black pepper leaf mediated green synthesis of silver nanoparticles and the antimicrobial study. Applied Nanoscience. 2013; 4(7): 809-818. doi: 10.1007/s13204-013-0260-7
7. Kastner C, Thunemann F. Catalytic reduction of 4-nitrophenol using silver nanoparticles with adjustable activity. Langmuir. 2016; 32(29): 7383-7391. doi: 10.1021/acs.langmuir.6b01477
8. Lin S, Huang R, Cheng W, et al. Silver nanoparticle-alginate composite beads for point-of-use drinking water disinfection. Water Research. 2013; 47(12): 3959-3965. doi: 10.1016/j.watres.2012.09.005
9. Mthombeni NH, Mpenyana-Monytasi I, Onyango, MS, et al. Breakthrough analysis for water disinfection using silver nanoparticles coated resin beads in fixed-bed column. Journal of Hazardous Materials. 2012; 217-218: 133-140. doi: 10.1016/j.jhazmat.2012.03.004
10. Lv Y, Lou H, Wang Z, et al. Silver nanoparticle-decorated porous ceramic composite for water treatment. Journal of Membrane Science. 2009; 331(1-2): 50-56. doi: 10.1016/j.memsci.2009.01.007
11. Saha S, Pal A, Kundu S, et al. Photochemical green synthesis of calcium-alginate-stabilised Ag and Au nanoparticles and their catalytic application to 4-nitrophenol reduction. Langmuir. 2009; 26(4): 2885-2893. doi: 10.1021/la902950x
12. Martinez-Gómez F, Guerrero J, Matsuhiro B, et al. In vitro release of metformin hydrochloride from sodium alginate/polyvinyl alcohol hydrogels. Carbohydrate Polymers. 2017; 155: 182-191. doi: 10.1016/j.carbpol.2016.08.079
13. Albalwi H, El Fadl FIA, Ibrahim MM, et al. Catalytic activity of silver nanocomposite beads for degradation of basic dye: kinetic and isothermal study. Applied Organometallic Chemistry. 2021; 36(1). doi: 10.1002/aoc.6490
14. Fagieh TM, Bakhsh EM, Khan SB, et al. Alginate/banana waste beads supported metal nanoparticles for efficient water remediation. Polymers. 2021; 13(23): 4054-4071. doi: 10.3390/polym13234054
15. Wang Y, Lu Y. Sodium alginate-based functional materials towards sustainability applications: Water treatment and energy storage. Industrial Engineering and Chemistry Research. 2023; 62: 11279-11304. doi: 10.1021/acs.iecr.3c01082
16. Alomar A, Qassim T, AlNajjar Y, et al. Green nanotechnology and phytosynthesis of metallic nanoparticles: The green approach, mechanism, biomedical applications and challenges. World Scientific Annual Review of Functional Materials. 2024; 1: 2430001-2430023.
17. Deen GR, Alhannan F, Henari F, et al. Effects of different parts of the okra plant (Abelmoschus esculentus) on the phytosynthesis of silver nanoparticles: Evaluation of synthesis conditions, nonlinear optical and antibacterial properties. Nanomaterials. 2022; 12(23): 4174-4185. doi: 10.3390/nano12234174
18. Mostafa H, Airouyuwa JO, Maqsood S. A novel strategy for producing nanoparticles from date seeds and enhancing their phenolic content and antioxidant properties using ultrasound-assisted extraction: A multivariate based optimization study. Ultrasonics Sonochemistry. 2022; 87: 106017. doi: 10.1016/j.ultsonch.2022.106017
19. Khalid S, Khalid N, Khan RS, et al. A review on chemistry and pharmacology of Ajwa dates fruit and pit. Trends in Food Science & Technology. 2017; 63: 60-69. doi: 10.1016/j.tifs.2017.02.009
20. Eid N, Osmanova H, Natchez C, et al. Impact of palm date consumption on microbiota growth and large intestinal health: A randomized, controlled, cross-over human intervention study. British Journal of Nutrition. 2015; 114(8): 1226-1236. doi: 10.1017/s0007114515002780
21. Cao PL, Lu W, Mata A, et al. Egg-box model-based gelation of alginate and pectin: A review. Carbohydrate Polymers. 2020; 242: 116389. doi: 10.1016/j.carbpol.2020.116389
22. Gangula A, Podila R, Karanam L, et al. Catalytic reduction of 4-nitrophenol using biogenic gold and silver nanoparticles derived from Breynia rhamnoides. Langmuir. 2011; 27(24): 15268-15274. doi: 10.1021/la2034559
23. Jiang ZJ, Liu CY, Sun LW. Catalytic properties of silver nanoparticles supported on silica spheres. The Journal of Physical Chemistry B. 2005; 109(5): 1730-1735. doi: 10.1021/jp046032g
24. Kumar I, Gangwar C, Yaseen B, et al. Kinetic and mechanistic studies of the formation of silver nanoparticles by nicotinamide as a reducing agent. ACS Omega. 2022; 7(16): 13778-13788. doi: 10.1021/acsomega.2c00046
25. Khan SB, Ahmad S, Kamal T, et al. Metal nanoparticles decorated sodium alginate-carbon nitride composite beads as effective catalyst for the reduction of organic pollutants. International Journal of Biological Macromolecules. 2020; 164: 1087-1098. doi: 10.1016/j.ijbiomac.2020.07.091
26. Shimoga G, Palem RR, Lee SH, et al. Catalytic degradability of p-nitrophenol using ecofriendly silver nanoparticles. Metals. 2020; 10(12): 1661. doi: 10.3390/met10121661
27. Meija YR, Bogireddy NKR. Reduction of 4-nitrophenol using green-fabricated metal nanoparticles. RSC Advances. 2022;

12(29): 18661-18675. doi: 10.1039/d2ra02663e

28. Farazin A, Mohammadimehr M, Ghasemi AM, et al. Design, preparation and characterization of CS/PVA/SA hydrogels modified with mesoporous Ag_2O/SiO_2 and curcumin nanoparticles for green, biocompatible, and antibacterial biopolymer film. RSC Advances. 2021; 11(52): 32775-32791. doi: 10.1039/d1ra05153a
29. Cittrarasu V, Kaliannan D, Dharman K, et al. Green synthesis of selenium nanoparticles mediated from Ceropegia bulbosa Roxb extract and its cytotoxicity, antimicrobial, mosquitocidal and photocatalytic activities. Scientific Reports. 2021; 11(1): 1032-1046. doi: 10.1038/s41598-020-80327-9